Preparation of Multiblock Copolymers via Step-wise Addition of L-lactide and Trimethylene Carbonate

Mark Abubekerov, Junnian Wei, Kevin R. Swartz, Zhixin Xie, Qibing Pei, and Paula L. Diaconescu*

Department of Chemistry and Biochemistry, University of California, Los Angeles, CA 90095

ABSTRACT: Poly(L-lactide) (PLA) is a bioderived and biodegradable polymer that has limited applications due to its hard and brittle nature. Incorporation of 1,3-trimethylene carbonate into PLA, in a block copolymer fashion, improves the mechanical properties, while retaining the biodegradability of the polymer, and broadens its range of applications. However, the preparation of 1,3-trimethylene carbonate (TMC)/ L-lactide (LA) copolymers beyond those of diblock and triblock structures has not been reported with explanations focusing mostly on thermodynamic reasons that impede copolymerization of TMC after lactide. Our approach focuses on the preparation of multiblock copolymers via ring opening polymerization (ROP) of LA and TMC, in step-wise addition, by a ferrocene-chelating heteroscorpionate zinc complex, [[fc(PPh_2)(BH[(3,5-$Me)_2$pz]$_2$)]Zn(μ-OCH_2Ph)]$_2$ ([($fc^{P,B}$) Zn(μ-OCH_2Ph)]$_2$, fc = 1,1'-ferrocenediyl, pz = pyrazole). The preparation of up to pentablock copolymers, from various combinations of LA and TMC, was accomplished and the physical, thermal, and mechanical properties of the resulting copolymers evaluated.

Growing concerns over the environmental damage caused by petroleum-based plastic waste[1] and the associated health effects due to petroleum processing[2] necessitate a shift to environmentally benign commodity plastics.[3-6] As a result, biodegradable plastics obtained from bio-renewable sources, in particular poly(L-lactide) (PLA),[7, 8] have received much attention in the past decades.[3, 9-11] Currently, applications of PLA vary widely from specialty plastics in biomedical devices[12-15] to commodity plastics in food packaging.[14-16] The mechanical properties of PLA resemble those of polystyrene;[11] it is a hard material with good tensile strength and high modulus.[10] Unfortunately, due to its low toughness, its overall applications are limited.[17] A potential way of enhancing the toughness of PLA is through copolymerization with 1,3-trimethylene carbonate (TMC), which gives a soft and amorphous homopolymer.[18] In this regard, both Guerin *et al.*[19] and Leng *et al.*[20] performed extensive studies on the influence of block TMC incorporation into PLA. These reports concluded that a ca. 20% weight of TMC into TMC/LA block copolymers is optimal. The resulting thermoplastic elastomers,[19, 20] of PLA-*b*-PTMC and PLA-*b*-PTMC-*b*-PLA compositions,[19] were shown to display both moderate elongation at break and moderate Young's modulus values. However, these copolymers were always prepared via initial TMC polymerization followed by sequential addition of LA, in the presence of various organic and metal-based catalysts,[19-29] but not the reverse. As a result, only a small number of LA/TMC block combinations in copolymers have been investigated and the influence of the more complicated block structures on the mechanical properties of these polymers are rather underexplored.[19] In the course of studying the redox switchable reactivity[30-44] of the ferrocene-chelating heteroscorpionate zinc complex, [[fc(PPh_2)(BH[(3,5-$Me)_2$pz]$_2$)]Zn(μ-OCH_2Ph)]$_2$ ([($fc^{P,B}$) Zn(μ-OCH_2Ph)]$_2$),[35] toward various monomers, we discovered that it can perform the ring opening polymerization (ROP) of LA and TMC regardless of the addition order. Based on our interest in the ROP of cyclic esters and carbonates, we set out to prepare multiblock copolymers of L-lactide and 1,3-trimethylene carbonate to examine their physical, thermal, and mechanical properties.

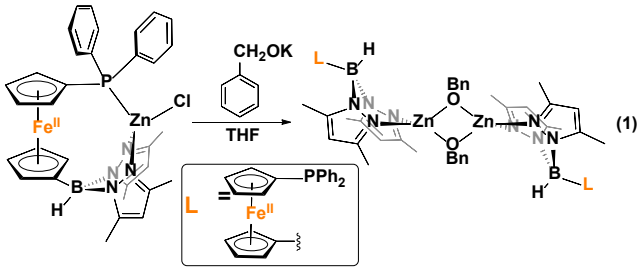

Because of the unique behavior of [($fc^{P,B}$)Zn(μ-OCH_2Ph)] toward the ROP of LA and TMC, we began by studying the solid-state structure and the solution behavior of the complex. The isolation of [($fc^{P,B}$)Zn(μ-OCH_2Ph)]$_2$ as yellow crystals in 63.0% yield (Eq 1) was achieved via the addition of ($fc^{P,B}$)ZnCl·(C_7H_8)[35] to in situ generated $KOCH_2Ph$ in THF. The solid-state molecular structure of

[(fc^{P,B})Zn(μ-OCH$_2$Ph)]$_2$ was determined using single-crystal X-ray diffraction (Figure 1). The coordination environment around each zinc center is a distorted tetrahedron (τ = 0.75).[45] The supporting ligands are bound in a κ^2 fashion via the pyrazole nitrogens, while the phosphine moieties are not coordinated, and the benzoxide groups are in a bridging position between the two metal centers.

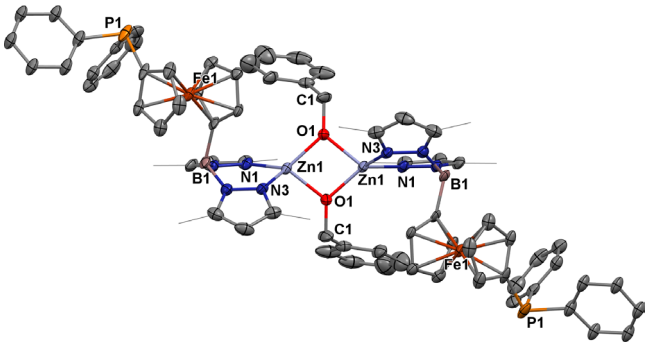

Figure 1. Molecular structure drawing of [(fc^{P,B})Zn(μ-OCH$_2$Ph)]$_2$ with thermal ellipsoids at 50% probability; hydrogen atoms and disordered counterparts are omitted for clarity.

In solution, a single species is observed by NMR spectroscopy (Figures S1-S4), with the resonance signals similar to those of previously reported (fc^{P,B})Zn complexes.[35] For example, the ^{31}P[^{1}H] NMR spectrum of [(fc^{P,B})Zn(μ-OCH$_2$Ph)]$_2$ shows a singlet at δ = -15.5 ppm. Similar chemical shifts of δ = -16.4 and -15.5 ppm were observed for a coordinated phosphine in (fc^{P,B})ZnCl and a free phosphine in fc(PPh$_2$)[B(OMe$_3$)$_2$], respectively.[35] Such minor differences in the ^{31}P[^{1}H] NMR spectra between free and zinc(II)-coordinated phosphines are commonly observed and are attributed to weak interactions between the soft phosphine ligands and the oxophilic zinc(II) centers.[46] Diffusion ordered spectroscopy (DOSY) NMR[47] experiments were conducted with (fc^{P,B})ZnCl and [(fc^{P,B})Zn(μ-OCH$_2$Ph)]$_2$ (Figures S10 and S11) to determine if the latter exists as a dimer in solution. Based on the Stokes-Einstein relationship,[47] the ratio of the radii of [(fc^{P,B})Zn(μ-OCH$_2$Ph)]$_2$ to (fc^{P,B})ZnCl is 1.63. This value is somewhat below the expected value of 2 for the dimer, as derived from the comparison of volumes from the solid-state structures. However, the ^{1}H Nuclear Overhauser Effect Spectroscopy (NOESY) NMR spectrum of [(fc^{P,B})Zn(μ-OCH$_2$Ph)]$_2$ shows a binding motif similar to that observed in the solid stare structure. Interactions between the protons of the pyrazole methyl groups and the benzoxide ligand are observed in the 2D plot, while the interactions between the phosphine phenyl groups and the benzoxide are not observed (Figures S6 and S7). Additionally, a variable temperature NMR study was performed. The spectra of [(fc^{P,B})Zn(μ-OCH$_2$Ph)]$_2$ show no significant changes in the range of 298 – 352 K (Figure S5), suggesting that the speciation of the complex remains the same in solution even at elevated temperatures.

The stability of [(fc^{P,B})Zn(μ-OCH$_2$Ph)]$_2$ was evaluated both in the presence and absence of monomer. In the absence of a monomer, [(fc^{P,B})Zn(μ-OCH$_2$Ph)]$_2$ slowly decomposes in benzene at ambient temperature, reaching 7.0% decomposition after 24 h (Figure S17). Heating the complex at 100 °C in benzene results in 34% decomposition after 1.5 h (Figure S18). However, in the presence of a monomer, no decomposition is observed, even at elevated temperatures (yy) for xx h (Figure S19).

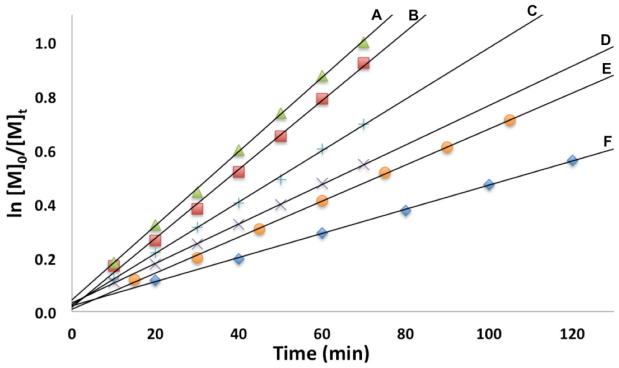

Figure 2. Semilogorithmic plots of L-lactide conversion with time in C$_6$H$_6$ at 70 °C with [(fc^{P,B})Zn(μ-OCH$_2$Ph)]$_2$ as a catalyst ([LA]$_0$ = 0.313 M: **A**, [Zn] = 4.69 mM, [LA]/[Zn] = 67; **B**, [Zn] = 3.91 mM, [LA]/[Zn] = 80; **C**, [Zn] = 3.13 mM, [LA]/[Zn] = 100; **D**, [Zn] = 2.34 mM, [LA]/[Zn] = 133; **E**, [Zn] = 1.88 mM, [LA]/[Zn] = 167; **F**, [Zn] = 1.56 mM, [LA]/[Zn] = 200).

Next, we looked at the identity of the catalytically active species in the case of each monomer. In order to evaluate if the catalytically active species remains a dimer, an attempt to characterize the product corresponding to the ring-opening of a single equivalent of monomer was made. Due to its slow rate of polymerization at ambient temperature, L-lactide was chosen as the model substrate. On an NMR scale, addition of one equivalent of L-lactide to [(fc^{P,B})Zn(μ-OCH$_2$Ph)]$_2$ resulted in the formation of a single major species (Figure S8) after 2 h hours at ambient temperature. Performing a DOSY NMR experiment on this product yielded a slower diffusion rate than for the parent complex (Figure S12), consistent with the retention of the dimeric state post incorporation of one equivalent of L-lactide per metal center. These results are reproduced during quenching experiments of L-lactide polymerizations. A DOSY experiment performed with [(fc^{P,B})Zn(PLA)$_{36}$(OCH$_2$Ph)]$_2$ yielded a diffusion rate of 1.04 × 10^{-6} m/s^2 (Figure S15). Water was then introduced into the same sample resulting in the hydrolysis of the polymer chains from the zinc catalyst. The free polymers, PhCH$_2$O(PLA)$_{36}$H, displayed a diffusion rate of 2.00 × 10^{-6} m/s^2 (Figure S16). This doubling of the diffusion rate upon hydrolysis of the active polymerization species is consistent with the liberation of polymer chains from a dimeric species. Similar results are obtained in the case of

TMC polymerization (Figures S13 and S14) suggesting that the catalytically active species is a dimer in both cases.

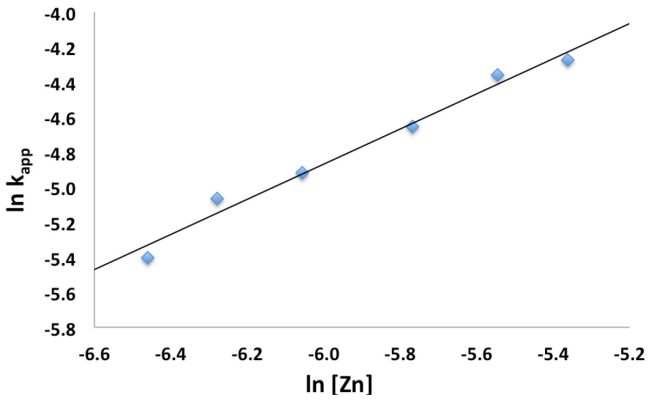

Figure 3. Plot of ln k_{app} vs. ln [Zn] for the polymerization of L-lactide with $[(fc^{P,B})Zn(\mu\text{-}OCH_2Ph)]_2$ as a catalyst (C_6H_6, 70 °C, $[LA]_o$ = 0.313 M).

The conversion of L-lactide was monitored for varying concentrations of monomer, in benzene at 70 °C by ^{1}H NMR spectroscopy. In all cases, first-order kinetics are observed via the semilogarithmic plots of several polymerizations (Figure 2). The order in pre-catalyst was determined via the logarithmic plot of the metal complex concentration against k_{app} (Figure 3) displaying first-order kinetics and yielding the following rate law:

$$-d[LA]/dt = k[Zn]^1[LA]^1 \qquad (2)$$

A first-order in both monomer and pre-catalyst is commonly observed for metal mediated ring-opening polymerizations. In particular, a clear order in catalyst is consistent with a well-behaved system in solution and the retention of the dimeric state by the catalyst throughout the polymerization process.[48, 49]

Finally, we looked at the preparation of LA/TMC homopolymers as well as, in keeping with the ca. 20% by weight optimal composition, the preparation of a variety of multiblock copolymers. In all cases, the multiblock copolymers were prepared via the sequential addition of monomer to the growing polymer chain. Utilizing our system, the copolymerization of TMC and LA is not limited by the order of monomer addition. The percent by weight composition of TMC was kept within 15-20%, and the number average molecular weight was kept at ca. 50,000 g/mol. We reasoned that attempting to maintain these variable relatively constant would allow us to probe the influence of microstructure on the physical properties of the corresponding materials.

Polymerization of ca. 100 equivalents of TMC (Table 1, entry 2) reaches completion at room temperature within one hour. Polymerization of L-lactide at room temperature is much slower and requires up to 24 hours for the same number of equivalents to reach completion. Raising the temperature to 70 °C results in a complete conversion within an hour. In both cases, the polymerizations are living. The molecular weights increase with conversion while retaining low dispersity values (Figures S30 and S31).

Table 1: Addition copolymerization of L-lactide and 1,3-trimethylene carbonate.

Entry	Polymer	PTMC (wt%)	PLA (wt%)	Mn (TMC, NMR)	Mn (LA, NMR)	Mn (NMR)	Mn (GPC)	*Đ*
1	PLA	-	100	-	-	40.7	39.8	1.14
2	PTMC	100	-	-	-	10.4	9.0	1.01
3	PLA-*b*-PTMC	19	81	10.0	43.7	53.7	55.5	1.12
4	PTMC-*b*-PLA	17	83	8.0	39.5	47.5	47.0	1.60
5	PTMC-*b*-PLA-*b*-PTMC	18	82	8.7	40.8	49.5	43.2	1.67
6	PLA-*b*-PTMC-*b*-PLA	17	83	9.0	43.7	52.7	55.6	1.46
7	PLA-*b*-PTMC-*b*-PLA-*b*-PTMC	19	81	10.2	42.9	53.1	48.2	1.49
8	PTMC-*b*-PLA-*b*-PTMC-*b*-PLA-*b*-PTMC	18	82	9.8	45.2	55.0	58.9	1.49
9	PLA-*b*-PTMC-*b*-PLA-*b*-PTMC-*b*-PLA	19	81	10.0	42.3	52.3	53.2	1.69

Conditions: benzene as a solvent (1.5 mL) and hexamethylbenzene as an internal standard. All experiments were performed at 70 °C, except for those corresponding to entry 2 and the first blocks of entries 3, 5, 7, and 8, which were performed at ambient temperature. M_n are reported in 10^3 g/mol; $Đ = M_w/M_n$.

Although the homopolymerization of TMC proceeds quickly at ambient temperature, elevated temperatures are required to polymerize it after L-lactide due to the nature of the intermediate formed after the ring opening of lactide that features a five-membered chelate.[30] This difference in shifting the polymerization of TMC from room temperature, as in the case of PLA-*b*-PTMC (Table 1, entry 3) to elevated temperatures, as in the case of PTMC-*b*-PLA (Table 1, entry 4), manifests itself in the broadening of the molecular weight distributions (Figure 6). As a result, the dispersity ($Đ$) values are larger for the copolymers subjected to TMC polymerization at elevated temperatures, ranging from 1.45 to 1.7 (Table 1, entries 4-9), then for the polymers that are not (Table 1, entries 1-3).

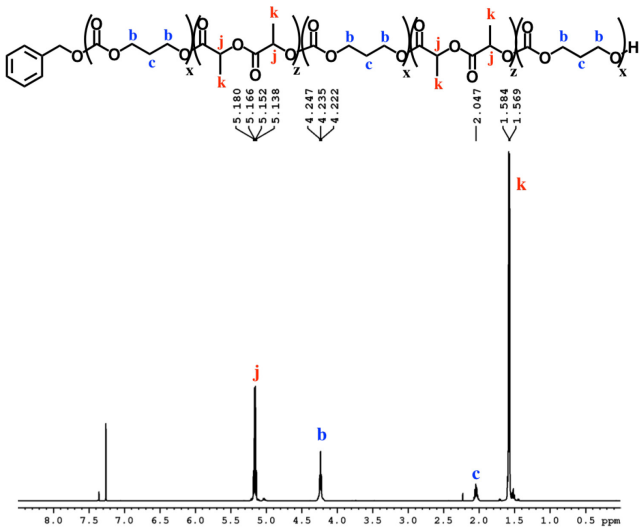

Figure 4. ^{1}H NMR spectrum ($CDCl_3$, 500 MHz, 298 K) of the PTMC-b-PLA-b-PTMC-b-PLA-b-PTMC copolymer.

The block structures of the polymers are consistent with observations from the ^{1}H NMR spectra. In all cases, the copolymers appear as mixtures of the corresponding homopolymers (Figures 4 and S22-S28), a defining characteristic of true block copolymers.[20] Alternatively, both gradient and random block copolymers of TMC and LA yield broadened peaks for PTMC and a distribution of peaks in the methine region of PLA.[20] The junctions of the copolymer[19, 50] can also be clearly observed in the ^{13}C NMR spectrum of the pentablock copolymers (Figures 5 and S29).[19, 20] The benzoxide end group is clearly observed in the DOSY spectra for both homopolymers, both in the case of the polymers still attached to the catalyst and in free polymers (Figures S13-S16). The downfield shift of the benzoxide methylene protons from 4.03 ppm in the parent complex to 4.72 ppm and 4.94 ppm in the ring-opening polymerization products of LA and TMC, respectively, is also indicative of the participation of the benzoxide group in the ring-opening process of the monomers.[19]

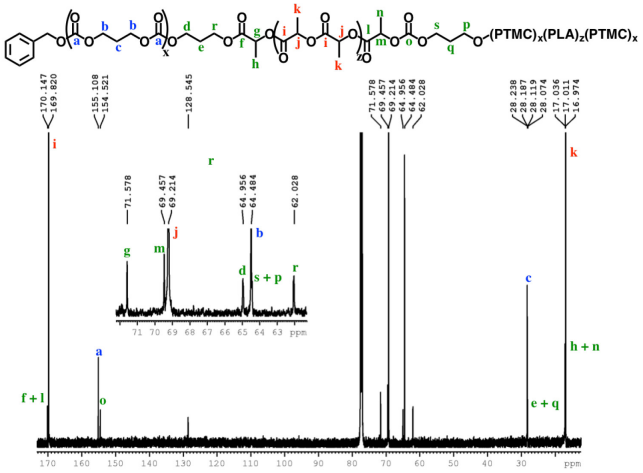

Figure 5. ^{13}C[H] NMR spectrum ($CDCl_3$, 500 MHz, 298 K) of the PTMC-b-PLA-b-PTMC-b-PLA-b-PTMC copolymer.

The differential scanning calorimetry (DSC) curves for the newly synthesized block copolymers display T_g and T_m values corresponding to isotactic PLA only (Table 2, Figures S41-Sy49. Even at high sample loadings, the T_g corresponding to PTMC (Figure S41) could not be detected, likely due to the relatively low content of PTMC in each copolymer. Only when we examined copolymers with a c.a. 40% by weight composition of TMC could we detect the T_g corresponding to PTMC (Table S2). In general, both the T_g and the T_m values are observed to decrease with the increasing number of blocks in the polymer. The mechanical properties of the polymers were determined via dynamic mechanical analysis (DMA) (Table 2, Figures S50-S57) on multiple samples of each copolymer prepared via a solvent casting method. The PLA homopolymer displayed a Young's modulus of 265 MPa and an elongation at break value of 16% (Table 2, entry 1). The copolymers display similar or better Young's modulus values and in most cases display an order of magnitude improved elongation at break values. The diblock copolymers showed a higher Young's modulus and a minor improvement in the elongation at break of up to ca. 40% (Table 2, entries 2-3). As the number of blocks increases to three or more, we observed a decrease in the Young's modulus; the Young's modulus values began resembling those of the homopolymer while the elongation at break values were drastically improved up to ca. 250% (Table 2, entries 4-8).

An inverse relationship between the Young's Modulus and elongation at break was observed by Guerin et. al.

upon increasing the percent composition of TMC in their copolymers.[19] We also prepared several triblock copolymers with varying percent compositions of TMC (Tables S1 and S2) to study the effects of varying TMC concentration in our copolymers. Lowering the TMC percent composition to 10% yielded a brittle material similar to PLA but with a higher Young's modulus than that of the homopolymer. On the other hand, when the TMC composition in the copolymer was increased to ca. 30% and 40% by weight we observed a similar inverse relationship between the Young's modulus and the elongation at break of the materials. Based on these results, a further increase in the PTMC composition would have a further negative impact on the materials Young's modulus at the expense of an increased elongation at break.

Table 2: Polymer thermal and physical properties.

Entry	Polymer Structure	T_g[a] (°C)	T_m[a] (°C)	E[b] (MPa)	σ[c] (MPa)	ε[d] (%)
1	PLA	55	173	265 ± 76	64 ± 3	16 ± 6
2	PLA-*b*-PTMC	42	173	551 ± 136	44 ± 1	40 ± 12
3	PTMC-*b*-PLA	37	164	537 ± 113	32 ± 6	19 ± 4
4	PTMC-*b*-PLA-*b*-PTMC	35	161	521 ± 30	24 ± 2	249 ± 32
5	PLA-*b*-PTMC-*b*-PLA	35	165	382 ± 61	12 ± 4	219 ± 44
6	PLA-*b*-PTMC-*b*-PLA-*b*-PTMC	34	165	471 ± 147	27 ± 0	208 ± 47
7	PTMC-*b*-PLA-*b*-PTMC-*b*-PLA-*b*-PTMC	34	160	334 ± 70	21 ± 2	176 ± 23
8	PLA-*b*-PTMC-*b*-PLA-*b*-PTMC-*b*-PLA	34	153	303 ± 44	20 ± 1	251 ± 32

[a] Glass transition temperatures and melting points were determined using DSC. [b] Young's modulus. [c] Ultimate tensile strength. [d] Elongation at break.

To gain a better understanding of the mechanism, we turned to density functional theory. All calculations were carried out with the GAUSSIAN09 program package[51] on the Extreme Science and Engineering Discovery Environment (XSEDE).[52] The methyl groups on the pyrazole substituents were replaced by hydrogen atoms and the phenyl groups on PPh_2 were replaced by methyl groups to simplify the calculation (for more details about calculations, see the supporting information). First, possible monomeric and dimeric structures of the zinc benzoxide complexes were optimized and their energies compared (Figure S72). The energy of dimer $[(fc^{P,B})Zn(\mu\text{-}OCH_2Ph)]_2$ was lower (by 3.3 kcal/mol) than of the corresponding monomer, $(fc^{P,B})Zn(OCH_2Ph)$, in agreement with the experimental observations.

Since the energy difference between the dimeric and the monomeric species was small, the free energy surfaces for the reaction with LA and TMC were thus computed for both the monomer and the dimer (Figures S73 and S74) to compare the initiation step. For LA, although the monomer shows a lower activation barrier than the dimer (by 2.7 kcal/mol) for the alkoxide nucleophilic attack ($TS_{I\text{-}II}$), the energy for the ring opening step ($TS_{II\text{-}III}$) and the overall activation barrier are lower for the dimeric species than for the monomer by 4.2 and 4.4 kcal/mol, respectively; furthermore, the two zinc centers participate in the process synergistically when the reaction occurs with the dimer. The initiation of TMC, both activation barriers were lower for the dimer (by 3.1 and 1.6 kcal/mol). These results are again in agreement with the experimental observations discussed above, that the dimeric zinc complex facilitates the polymerization.

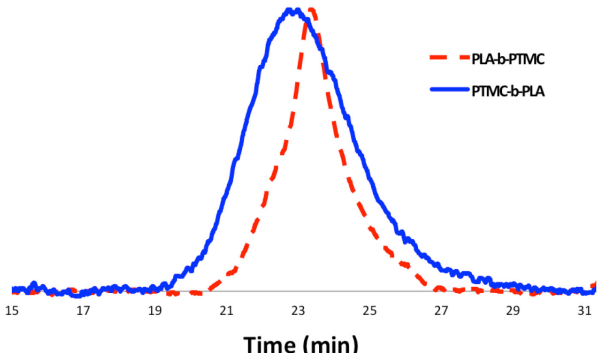

Figure 6. GPC traces of the PLA-*b*-PTMC (table 1, entry 3) and PTMC-*b*-PLA (table 1, entry 4) copolymers.

The copolymerization steps were then considered. Since the insertion of TMC leads to a product that has a similar structure as the step before, each following insertion should be similar to the initiation step, making the homo-polymerization and co-polymerization possible. However, after the insertion of LA, the resulting product contains a five-membered ring, in which the bond between the Zn center and the carbonyl group cannot be ignored. Thus, the insertions of a second LA or TMC molecule, respectively, after the insertion of the first LA were considered. As shown in Figure 7, the dimeric species significantly lowers the overall activation barriers, thus making the propagations possible after the insertion of LA. We would like to note that we are treating the results shown in Figure 7 from a qualitative point of view that allows us to compare the behavior of LA versus TMC. The large number of atoms involved and the simplifications necessary in order to get the respective transition states and intermediates to converge in a reasonable amount of time likely resulted in obtaining energies for the products that are positive with respect to the starting materials.

It is interesting to observe that after the insertion of LA, the insertion of another LA is easier than the insertion of TMC. Based on these results, we can envision that although the homopolymerization of TMC is much easier than LA, however, if we do the co-polymerization together with LA and TMC in one-pot, the LA would be consumed first (Figure S70).

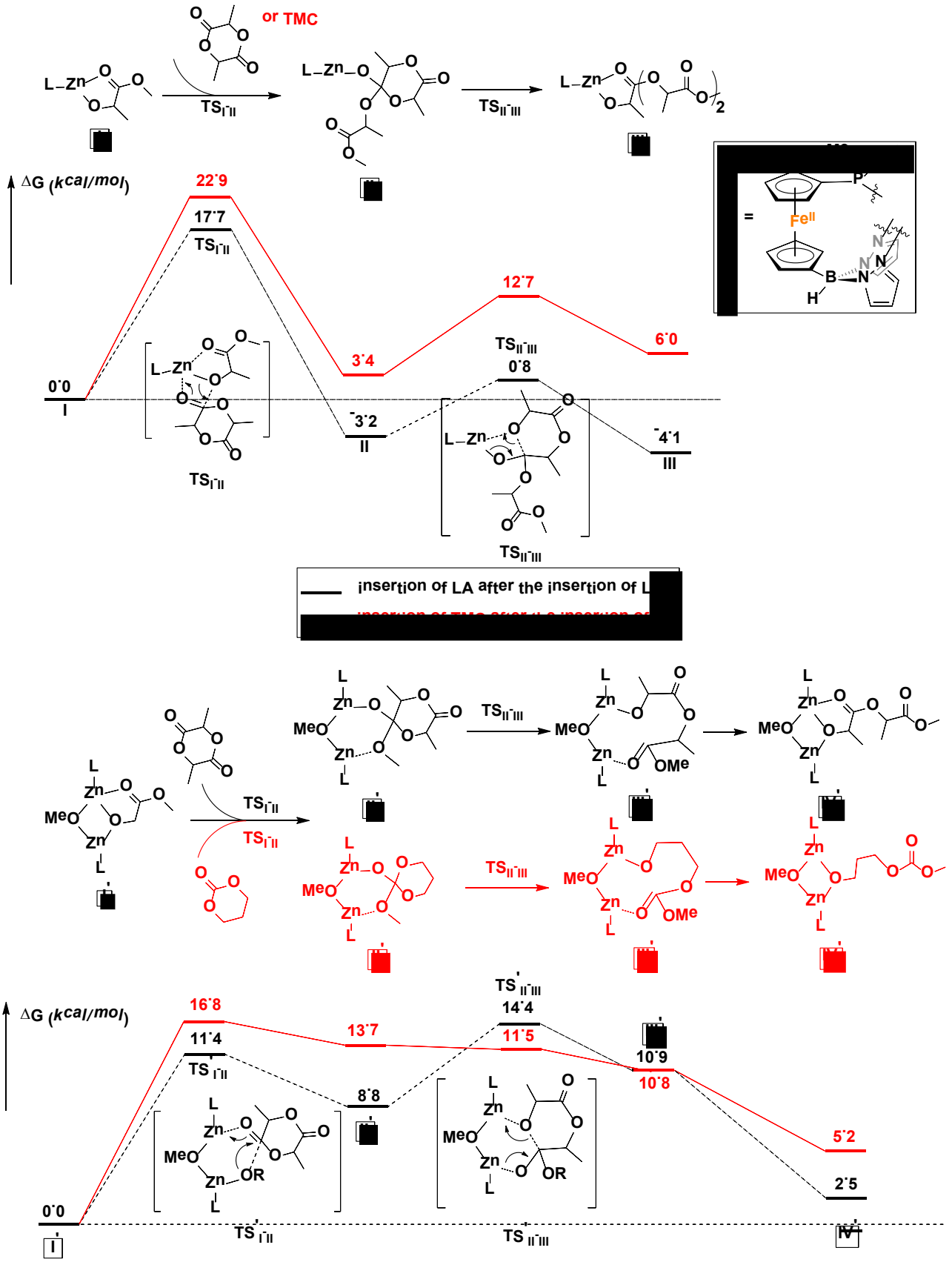

Figure 7. Comparison of reaction coordinates for propagation catalyzed by a monomeric (top) or dimeric (bottom) form of the zinc complex.

In conclusion, we thoroughly investigated the solution state behavior of $[(fc^{P,B})Zn(\mu\text{-}OCH_2Ph)]_2$ in the presence and absence of LA and TMC. The zinc complex was found to react as a dimer when catalyzing the ROP of L-lactide and 1,3-trimethylene carbonate. Surprisingly, the preparation of various multiblock copolymers could be achieved via a simple step-wise addition of the cyclic ester and carbonate in the presence of the catalyst. The physical, thermal, and mechanical properties of the isolated polymers were determined via NMR spectroscopy, GPC, DSC, and DMA. The reasons behind the unique polymerization activity of the $[(fc^{P,B})Zn(\mu\text{-}OCH_2Ph)]_2$ complex are currently under investigation.

References

1. M. R. Gregory, *Phil. Trans. R. Soc. B*, 2009, **364**, 2013-2025.
2. R. U. Halden, *Annu. Rev. Public Health*, 2010, **31**, 179-194.
3. G.-Q. Chen and M. K. Patel, *Chem. Rev.*, 2012, **112**, 2082-2099.
4. J.-C. Bogaert and P. Coszach, *Macromol. Symp.*, 2000, **153**, 287-303.
5. R. E. Drumright, P. R. Gruber and D. E. Henton, *Adv. Mater.*, 2000, **12**, 1841-1846.
6. Y. Zhu, C. Romain and C. K. Williams, *Nature*, 2016, **540**, 354-362.
7. J. Lunt, *Polym. Degrad. Stab.*, 1998, **59**, 145-152.
8. E. T. H. Vink, K. R. Rábago, D. A. Glassner and P. R. Gruber, *Polym. Degrad. Stab.*, 2003, **80**, 403-419.
9. O. Dechy-Cabaret, B. Martin-Vaca and D. Bourissou, *Chem. Rev.*, 2004, **104**, 6147-6176.
10. L. S. Nair and C. T. Laurencin, *Prog. Polym. Sci.*, 2007, **32**, 762-798.
11. R. H. Platel, L. M. Hodgson and C. K. Williams, *Polym. Rev.*, 2008, **48**, 11-63.
12. T. Hayashi, *Prog. Polym. Sci.*, 1994, **19**, 663-702.
13. J. C. Middleton and A. J. Tipton, *Biomaterials*, 2000, **21**, 2335-2346.
14. Y. Ikada and H. Tsuji, *Macromol. Rapid Commun.*, 2000, **21**, 117-132.
15. W. Amass, A. Amass and B. Tighe, *Polym. Int.*, 1998, **47**, 89-144.
16. E. Chiellini and R. Solaro, *Adv. Mater.*, 1996, **8**, 305-313.
17. J. M. Becker, R. J. Pounder and A. P. Dove, *Macromol. Rapid Commun.*, 2010, **31**, 1923-1937.
18. A. P. Pêgo, D. W. Grijpma and J. Feijen, *Polymer*, 2003, **44**, 6495-6504.
19. W. Guerin, M. Helou, J.-F. Carpentier, M. Slawinski, J.-M. Brusson and S. M. Guillaume, *Polym. Chem.*, 2013, **4**, 1095-1106.
20. X. Leng, Z. Wei, Y. Ren, Y. Bian, Q. Wang and Y. Li, *RSC Adv.*, 2016, **6**, 40371-40382.
21. Y. Lemmouchi, M. C. Perry, A. J. Amass, K. Chakraborty and E. Schacht, *J. Polym. Sci. A Polym. Chem.*, 2008, **46**, 5348-5362.
22. D. J. Darensbourg, W. Choi, O. Karroonnirun and N. Bhuvanesh, *Macromolecules*, 2008, **41**, 3493-3502.
23. Y. Nakayama, H. Yasuda, K. Yamamoto, C. Tsutsumi, R. Jerome and P. Lecomte, *React. Funct. Polym.*, 2005, **63**, 95-105.
24. D. W. Grijpma, C. A. P. Joziasse and A. J. Pennings, *Macromol. Rapid Commun.*, 1993, **14**, 155-161.
25. J.-H. Kim, S. Y. Lee and D. J. Chung, *Polym. J.*, 2000, **32**, 1056-1059.
26. D. Pospiech, H. Komber, D. Jehnichen, L. Häussler, K. Eckstein, H. Scheibner, A. Janke, H. R. Kricheldorf and O. Petermann, *Biomacromolecules*, 2005, **6**, 439-446.
27. T. Tyson, A. Finne-Wistrand and A.-C. Albertsson, *Biomacromolecules*, 2009, **10**, 149-154.
28. H. R. Kricheldorf and S. Rost, *Macromolecules*, 2005, **38**, 8220-8226.
29. L. Wang, C. E. Kefalidis, S. Sinbandhit, V. Dorcet, J.-F. Carpentier, L. Maron and Y. Sarazin, *Chem. Eur. J.*, 2013, **19**, 13463-13478.
30. J. Wei, M. N. Riffel and P. L. Diaconescu, *Macromolecules*, 2017, **50**, 1847-1861.
31. S. M. Shepard and P. L. Diaconescu, *Organometallics*, 2016, **35**, 2446–2453.
32. S. M. Quan, X. Wang, R. Zhang and P. L. Diaconescu, *Macromolecules*, 2016, **49**, 6768-6778.
33. W. Huang and P. L. Diaconescu, *Inorg. Chem.*, 2016, **55**, 10013–10023.
34. M. Abubekerov, S. M. Shepard and P. L. Diaconescu, *Eur. J. Inorg. Chem.*, 2016, **2016**, 2634-2640.
35. M. Abubekerov and P. L. Diaconescu, *Inorg. Chem.*, 2015, **54**, 1778–1784.
36. X. Wang, A. Thevenon, J. L. Brosmer, I. Yu, S. I. Khan, P. Mehrkhodavandi and P. L. Diaconescu, *J. Am. Chem. Soc.*, 2014, **136**, 11264-11267.
37. E. M. Broderick, N. Guo, T. Wu, C. S. Vogel, C. Xu, J. Sutter, J. T. Miller, K. Meyer, T. Cantat and P. L. Diaconescu, *Chem. Commun.*, 2011, **47**, 9897-9899.
38. E. M. Broderick, N. Guo, C. S. Vogel, C. Xu, J. Sutter, J. T. Miller, K. Meyer, P. Mehrkhodavandi and P. L. Diaconescu, *J. Am. Chem. Soc.*, 2011, **133**, 9278–9281.
39. A. B. Biernesser, K. R. Delle Chiaie, J. B. Curley and J. A. Byers, *Angew. Chem. Int. Ed.*, 2016, **55**, 5251–5254.
40. A. B. Biernesser, B. Li and J. A. Byers, *J. Am. Chem. Soc.*, 2013, **135**, 16553-16560.
41. C. Hermans, W. Rong, T. P. Spaniol and J. Okuda, *Dalton Trans.*, 2016, **45**, 8127-8133.
42. A. Sauer, J.-C. Buffet, T. P. Spaniol, H. Nagae, K. Mashima and J. Okuda, *ChemCatChem*, 2013, **5**, 1088-1091.
43. A. J. Teator, D. N. Lastovickova and C. W. Bielawski, *Chem. Rev.*, 2016, **116**, 1969-1992.
44. A. G. Tennyson, V. M. Lynch and C. W. Bielawski, *J. Am. Chem. Soc.*, 2010, **132**, 9420-9429.
45. L. Yang, D. R. Powell and R. P. Houser, *Dalton Trans.*, 2007, DOI: 10.1039/B617136B, 955-964.

46. C. Fliedel, V. Rosa, F. M. Alves, A. M. Martins, T. Aviles and S. Dagorne, *Dalton Trans.*, 2015, **44**, 12376-12387.
47. D. Li, G. Kagan, R. Hopson and P. G. Williard, *J. Am. Chem. Soc.*, 2009, **131**, 5627-5634.
48. B. M. Chamberlain, M. Cheng, D. R. Moore, T. M. Ovitt, E. B. Lobkovsky and G. W. Coates, *J. Am. Chem. Soc.*, 2001, **123**, 3229-3238.
49. T. Ouhadi, A. Hamitou, R. Jerome and P. Teyssie, *Macromolecules*, 1976, **9**, 927-931.
50. P. Dobrzynski and J. Kasperczyk, *J. Polym. Sci. A Polym. Chem.*, 2006, **44**, 3184-3201.
51. M. J. Frisch, *Journal*, 2010 (see the SI for the full reference).
52. J. Towns, T. Cockerill, M. Dahan, I. Foster, K. Gaither, A. Grimshaw, V. Hazlewood, S. Lathrop, D. Lifka, G. D. Peterson, R. Roskies, J. R. Scott and N. Wilkens-Diehr, *Journal*, 2014, **16**, 62-74.

TOC graphic